Gain and stability in photorefractive two-wave mixing

Ivan de Oliveira and Jaime Frejlich
Laboratório de Óptica, IFGW, UNICAMP, Campinas, São Paulo, Brazil
(Received 27 October 2000; published 13 August 2001)

We demonstrate that the negative amplitude gain in a photorefractive two-wave-mixing experiment under applied electric field measurably reduces the characteristic instability of the recorded hologram. In this sense photorefractive materials behave like electronic amplifiers with feedback. We analyze the case of stationary and running holograms both under an externally applied electric field. A continuous phase-modulation method is used to simultaneously measure diffraction efficiency and phase shift. Measurements carried out on a $Bi_{12}TiO_{20}$ crystal at 514.5 nm wavelength confirm the occurrence of continuous oscillations in both the diffraction efficiency and the phase shift. The perturbations in the diffraction efficiency increase considerably with increasing applied field and are reduced when energy is transferred from the weaker to the stronger beam (negative gain). Our results indicate that the perturbations in our experiments are probably due to resonantly excited transient effects.

DOI: 10.1103/PhysRevA.64.033806 PACS number(s): 42.60.Lh, 42.65.Hw, 42.40.Ht, 42.40.Pa

I. INTRODUCTION

Photorefractives are photoconductive and electro-optic materials where electrons (and/or holes) may be excited, by the action of light, from photoactive centers into the conduction (valence) band. These electrons move by diffusion or by the action of an applied electric field and are retrapped somewhere else. If a nonuniform pattern of light is projected onto the sample a correspondingly nonuniform spatial distribution of charges arises with an associated space-charge electric field, which gives rise to an index-of-refraction modulation via the electro-optic effect. In this way an index-of-refraction modulation is produced when a pattern of fringes of light of the form

$$I=|R+S|^2=(I_R+I_S)[1+|m|\cos(Kx+\phi)], \tag{1}$$

arising from the interference of two coherent beams of complex amplitudes $S=|S|e^{-i\psi_S}$ and $R=|R|e^{-i\psi_R}$, is projected onto a photorefractive material [1–4]. Here $I_R=|R|^2$ and $I_S=|S|^2$ are the corresponding irradiances of the incident beams, $K=2\pi/\Delta$ is the value of the vector $\vec{K}$, directed along the x coordinate, with Δ being the fringes' spatial period, $m=2S^*R/(|S|^2+|R|^2)$ is the pattern-of-fringes complex modulation depth, and $\phi=\psi_S-\psi_R$. The resulting index-of-refraction modulation has the same $\vec{K}$ but is ϕ_p phase shifted from the pattern of light [4,5]. This index-of-refraction modulation in the whole volume represents a reversible volume phase hologram which produces amplitude and phase coupling between the interfering recording beams [6,7]. Such a coupling results in a feedback between the pattern of fringes and the reversibly recorded hologram, a process known as self-diffraction. The amplitude coupling does in fact represent a transfer of energy from one beam to the other and is described by the equations [4,6]

$$I_S(d)=I_S(0)\,\frac{1+\beta^2}{1+\beta^2 e^{-\Gamma d/2}}, \tag{2}$$

$$I_R(d)=I_R(0)\,\frac{1+\beta^2}{\beta^2+e^{\Gamma d/2}}, \tag{3}$$

where Γ and γ are [4,5]

$$\Gamma\propto \mathrm{Im}\{\kappa\},\quad \gamma\propto \mathrm{Re}\{\kappa\}. \tag{4}$$

Here (0) and (d) indicate the input ($z=0$) and output ($z=d$) positions inside the crystal with $\beta^2=I_R(0)/I_S(0)$, Im{ } and Re{ } stand for the imaginary and real parts, respectively, and κ is the coupling constant as defined in the dynamic coupled-wave theory [4,5]. This κ depends on the externally applied field E_0 as well as on material and experimental parameters and fully characterizes the nature of the dynamic hologram being recorded, including the value of ϕ_p that is computed from [4,5]

$$\tan\phi_p=\frac{\mathrm{Im}\{\kappa\}}{\mathrm{Re}\{\kappa\}}=\frac{\Gamma}{\gamma}. \tag{5}$$

The coupling between the phases of the interfering beams produces a bending or tilting of the hologram and is described by [4,5]

$$\psi_S(d)-\psi_R(d)=\psi_S(0)-\psi_R(0)+\frac{1}{2\tan\phi_p}\ln\frac{(\beta^2+e^{\Gamma d})^2}{(1+\beta^2)^2e^{\Gamma d}}. \tag{6}$$

The diffraction efficiency η and the phase shift φ between the transmitted and diffracted beams along any one of the two directions behind the crystal are formulated, respectively, by [4,5]

$$\eta=\frac{2\beta^2}{1+\beta^2}\,\frac{\cosh(\Gamma d/2)-\cos(\gamma d/2)}{\beta^2e^{-\Gamma d/2}+e^{\Gamma d/2}}, \tag{7}$$

$$\tan\varphi = \frac{\sin(\gamma d/2)}{[(1-\beta^2)/(1+\beta^2)][\cosh(\Gamma d/2)-\cos(\gamma d/2)]+\sinh(\Gamma d/2)}. \tag{8}$$

II. GAIN AND STABILITY: STEADY-STATE BEHAVIOR

Photorefractive holographic recording is a feedback process between the pattern of fringes and the index-of-refraction modulation. Feedback is the essential fact underlying self-diffraction (it has no relation to the already published [5,8,9] external feedback that uses an electronic circuit to stabilize the holographic recording) and is characterized by either a positive (energy being transferred from the stronger to the weaker beam) or a negative (energy transferred from the weaker to the stronger beam) gain process depending upon the direction of energy transfer. The signal may therefore be amplified as with electronic amplifiers. The two systems do not have an identical behavior, but a parallelism, in some aspects, can be established between holographic recording and the operation of electronic amplifiers. It is known that the latter exhibit a higher stability when operated in a negative feedback configuration [10] and we expect that photorefractive holograms may exhibit a similar behavior. In fact, let A represent the amplification of the electronic device and $\mathcal{B}$ the negative feedback, v_i and v_o being the input and output signals, respectively, so that we may write [10]

$$\frac{v_o}{v_i} = G = \frac{A}{1+\mathcal{B}A}, \tag{9}$$

where G represents the effective signal gain with feedback. For a negative feedback and a large amplification ($A\mathcal{B}\gg 1$) the gain simplifies to $G=1/\mathcal{B}$, which is independent of the device's characteristics (represented by A). This result means that perturbations arising from variation in the material parameters (intrinsic noise) of the amplifier are eliminated while it is operated in a negative feedback mode. External noises are amplified instead along with the input signal. However, if the amplification is not large enough (which is actually the case in this paper) the intrinsic noise will not be eliminated but correspondingly decreased.

It is known that photorefractive holograms produced under the action of an externally applied electric field exhibit comparatively large diffraction efficiencies but they are very noisy [11]. This noise may arise from the generation of resonantly moving holograms (or other causes) in the sample, which may be considered as internally generated noise. Accordingly these noises are expected to be reduced when operating in a negative feedback mode. The above general conclusions can be particularized for the case of photorefractive materials. To facilitate calculations we may assume that, whatever the origin of these internal noises may be, they can be attributed to variations in the parameters Γ and γ so that their relative effect on η and φ may be computed from Eqs. (7) and (8) as follows:

$$\left|\frac{1}{\eta}\frac{\partial\eta}{\partial\Gamma}\right| \approx \left|\frac{e^{\Gamma d/2}-\cos(\gamma d/2)}{\cosh(\Gamma d/2)-\cos(\gamma d/2)}\right|\frac{d}{2}, \tag{10}$$

$$\left|\frac{1}{\eta}\frac{\partial\eta}{\partial\gamma}\right| \approx \left|\frac{\sin(\gamma d/2)}{\cosh(\Gamma d/2)-\cos(\gamma d/2)}\right|\frac{d}{2}, \tag{11}$$

where the condition $\beta^2\gg 1$ was assumed. Equation (11) clearly shows that the sign of γ has no effect on the relative variation of η. However, the analysis of Eq. (10) shows that [except for $\Gamma d\Rightarrow 0$ with $\cos(\gamma d/2)\Rightarrow 0$] a negative ($\Gamma<0$) feedback may reduce the effect of Γ variations on η. The same calculation performed for φ in Eq. (8) does not lead to a conclusive result because it is too dependent upon the particular values of Γ and γ.

III. GAIN AND STABILITY: TRANSIENT BEHAVIOR

Negative feedback in electronic amplifiers also has important effects on the dynamics of the process: the temporal bandwidth is enlarged, which is to say that processes become faster. We expect a similar behavior for photorefractive holograms. Let us consider a strong (pump of irradiance I_R) and a weak (signal of irradiance I_S) beam such that $I_R\gg I_S$ (the so-called undepleted pump approximation), in which case the recording is described by [12,13]

$$\tau_{sc}\frac{\partial^2\Psi(z,t)}{\partial z\,\partial t}+\frac{\partial\Psi(z,t)}{\partial z}+i2\kappa\Psi(z,t)=0, \tag{12}$$

where Ψ represents either m or the conjugated complex signal amplitude S^*. The time is t, the position along the sample thickness is z, τ_{sc} is the characteristic hologram buildup time, and κ is the coupling constant referred to in Eq. (4). It can be shown [13] that the solution of Eq. (12) characterizes an amplification with feedback where the gain depends on κ. Following the procedure in [12,13] we shall look for a solution of Eq. (12) for the simple case of erasure of the signal S. In this case we shall make $\Psi(z,t)\rightarrow S^*(z,t)$ and look for a solution of the form

$$S^*(z,t)=S_0S_1(z,t)\exp(-t/\tau_{sc}), \tag{13}$$

which is shown to be

$$S^*(z,t)=S_0J_0(\sqrt{8i\kappa tz/\tau_{sc}\cos\theta})\exp(-t/\tau_{sc}), \tag{14}$$

where $J_0(\,)$ is the Bessel function of order zero, $i=\sqrt{-1}$, and $S_0=S^*(0,0)$. The coupled-wave theory shows that diffraction of the recording beams S and R results in energy transfer from one of these beams to the other. If a hologram is erased using the beam R, with energy being transferred from R to S, the erasure can be considered a positive feedback process. In fact, the signal beam S that originates from

the diffraction of the R beam during erasure is increased ("amplified") due to such energy transfer. The presence of the S beam reproduces the original recording pattern of fringes, so that some extent of hologram recording results and the erasure is slowed down. In the opposite case, if energy transfer occurs from S to R, there is a negative feedback and the hologram erasure is speeded up. The transfer of energy from one beam to the other is determined by the crystal parameters, that is to say, it is determined by the sign of κ. In conclusion, as for the case of amplifiers in electronic circuits, a photorefractive negative feedback produces a faster response, i.e., an increase of the frequency bandwidth results. This similarity between photorefractive two-wave mixing and electronic amplification has already been pointed out elsewhere [13]. The qualitative conclusions above may be confirmed using our mathematical results. Let us assume an erasure process where the weak beam is S, whose evolution is described by Eq. (14). The corresponding intensity evolution at the output $z=d$ is therefore given by

$$|S|^2=|S_0 J_0(\sqrt{8i\kappa td/\tau_{sc}\cos\theta})e^{-t/\tau_{sc}}|^2$$
$$=|S_0|^2|J_0(\sqrt{8i\kappa td/\tau_{sc}\cos\theta})|^2 e^{-t2\,\mathrm{Re}\{\tau_{sc}\}/|\tau_{sc}|^2}. \tag{15}$$

Figure 1 shows the numerical plot of $|S|^2$ from Eq. (15), in arbitrary units, for $|S_0|=1$ and some usual values for a bismuth titanate (BTO) crystal with $E_0/E_D=2$ and $K=12\ \mu\mathrm{m}^{-1}$: $\mathrm{Re}\{\tau_{sc}\}=0.4$ s and $\mathrm{Im}\{\tau_{sc}\}=-0.65$ s. The abscissa is always the normalized time $t/|\tau_{sc}|$. It is clear, from these four graphics in Fig. 1, that for any value of the γd parameter the erasure is always faster and less oscillating for lower values of Γd, a condition where the transfer of energy from the pump to the signal beam is reduced or even reversed.

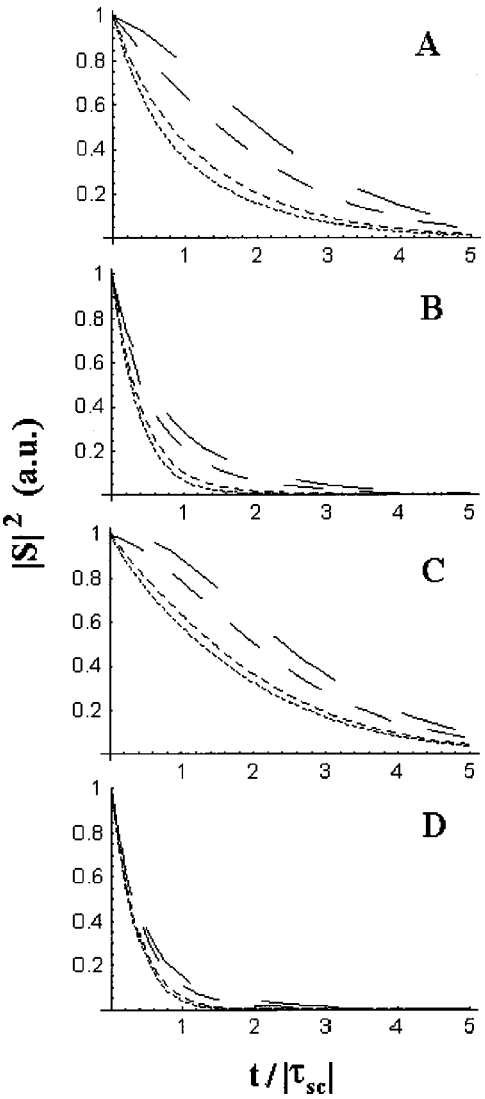

FIG. 1. Numerical plot of $|S|^2$ vs the normalized time $t/|\tau_{sc}|$, for $\mathrm{Re}\{\tau_{sc}\}=0.4$ s and $\mathrm{Im}\{\tau_{sc}\}=-0.65$ s: (a) for $\Gamma d=1$ with $\gamma d=-0.5$, -0.25, 0.25, and 0.5 from the smallest to the largest dashed lines, respectively; (b) for $\Gamma d=-1$ with $\gamma d=-0.5$, -0.25, 0.25, and 0.5 from the smallest to the largest dashed lines, respectively; (c) for $\gamma d=1$ with $\Gamma d=-0.5$, -0.25, 0.25, and 0.5 from the smallest to the largest dashed lines, respectively; (d) for $\gamma d=-1$ with $\Gamma d=-0.5$, -0.25, 0.25, and 0.5 from the smallest to the largest dashed lines, respectively.

IV. GAIN AND STABILITY IN RUNNING HOLOGRAMS

Photorefractive materials under externally applied dc electric field E_0 produce rather unstable stationary (nonmoving) holograms. A field is applied to increase the hologram diffraction efficiency [14] (because of its effect on κ) at the cost of increased instability [11]. Such instability has been long known and attributed to the beating between the recorded stationary hologram and the resonantly excited running holograms arising from perturbations in the experimental setup. In fact, a pattern of fringes moving along coordinate x with velocity v produces a space-charge field (and an associated index-of-refraction hologram) of the form $E_{sc}e^{iKx}$ which is ruled by the equation [11]

$$\tau_{sc}\frac{\partial E_{sc}}{\partial t}+E_{sc}=-mE_{\mathrm{eff}}e^{-iKvt}, \tag{16}$$

$$E_{\mathrm{eff}}=\frac{E_0+iE_D}{1+K^2l_s^2-iKl_E}, \tag{17}$$

$$\frac{1}{\tau_{sc}}=\omega_R+i\omega_I, \tag{18}$$

with

$$\omega_R=\mathrm{Re}\left\{\frac{1}{\tau_{sc}}\right\},\quad \omega_I=\mathrm{Im}\left\{\frac{1}{\tau_{sc}}\right\}. \tag{19}$$

The expressions

$$E_{sc}^{st}e^{iKx} = -m\frac{1}{\tau_M}\frac{E_0 + iE_D}{(1+K^2L_D^2 - iKL_E)(\omega_R + i\omega_I - iKv)} \times e^{i(Kx-Kvt)}, \tag{20}$$

$$E_{sc}^{trs}e^{iKx} = E_{sc}^{0}e^{-\omega_R t}e^{i(Kx-\omega_I t)} \tag{21}$$

are solutions of Eq. (16) that represent the steady-state and the transient running holograms, respectively. Here E_D is the space-charge field arising from diffusion and L_D, l_s, l_E, L_E, and τ_M are material parameters that are described in the literature [11]. The quantity Kv is the so-called two-wave-mixing detuning because it represents the difference in angular frequency between the interfering beams. In the presence of external perturbations transient holograms [see Eq. (21)] are repeatedly generated and their simultaneous presence with the steady-state running hologram [see Eq. (20)] moving with a different speed may be one of the causes of instability [11]. Other causes may be subharmonic generation [15–17] or other parametric excitation mechanisms [18,19], depending on the specific experimental conditions. In the present conditions our experimental results indicate, as will be seen below, that resonantly excited holograms of the type indicated by Eq. (21) are probably the main cause of instability. As for the case of stationary holograms, such instabilities should be reduced by operating in a negative feedback mode, a fact that was actually experimentally observed and reported below. It is worth pointing out that, although Eqs. (20) and (21) adequately describe the nature of these holograms, the overall result should take into account the fact that m is a function of the depth coordinate z. For moving holograms the influence of bulk absorption upon the relaxation time should also be considered [20]. Self-diffraction effects mathematically described by Eqs. (2)–(6) should also be accounted for.

V. EXPERIMENT

To analyze the instability dependence upon gain, a standard two-wave mixing experiment is carried out using a nominally undoped $Bi_{12}TiO_{20}$ crystal [21] 2.05 mm thick as depicted in Fig. 2. Two mutually coherent linearly polarized 514.5-nm-wavelength laser beams are expanded and symmetrically directed onto the (110) crystal input plane with irradiances I_R and I_S. The hologram vector $\vec{K}$ is parallel to the x coordinate axis and perpendicular to the [001] crystal axis. The external electric field is applied parallel to $\vec{K}$. The incident light polarization is chosen so that the transmitted and diffracted beams behind the crystal are parallel polarized [22]. Also, $\beta^2 = I_R/I_S \gg 1$ so as to have $|m| \ll 1$ in order to satisfy the first-spatial-harmonic approximation [23].

A. Diffraction efficiency and phase-shift measurement

The experiment requires the diffraction efficiency and the phase shift to be measured continuously without perturbing the recording process. For this purpose the use of the widespread probe-beam technique (an auxiliary low-power unexpanded beam shinning on the sample at the Bragg angle to measure η) is not adequate for three reasons: (a) it gives no information about the phase, (b) even a low-power 0.5-mW He-Ne laser affects the recording in BTO, and (c) for the relatively small spatial period here involved (about 0.5 μm in some of the experiments) and the present crystal thickness (about 2 mm), the angular Bragg selectivity [24] (about 0.2 mrad) is too restrictive for the usual angular divergence (1–2 mrad) of commercial He-Ne low-power lasers. The technique used in this experiment was phase modulation (with angular frequency $\Omega = 2\pi \times 2000$ rad/s and amplitude $\psi_d = 0.14$ rad) of one of the interfering beams (the pump in this case), which produces harmonic terms in the irradiance (I_S) behind the crystal. The first- and second-harmonic terms are measured using lock-in amplifiers, tuned to Ω (amplification A^{Ω}) and 2Ω (amplification $A^{2\Omega}$), respectively, and the corresponding output signals are [25]

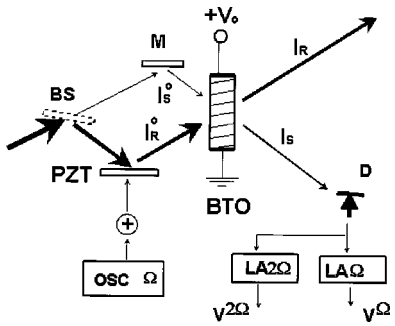

FIG. 2. Experimental setup: BS, beam splitter; M, mirror; I_S^0, incident signal beam; I_R^0 incident pump beam; I_R and I_S, two-wave-mixed pump and signal beams; BTO, photorefractive crystal; $+V_0$, applied voltage; PZT, piezoelectric-supported mirror; OSC, Ω oscillator; LA Ω and $LA2\Omega$, lock-in amplifiers tuned to Ω and 2Ω, respectively; D photodetector.

$$V^{\Omega} = A^{\Omega}K_d^{\Omega}2\psi_d\sqrt{I_S^t I_R^t}\sqrt{\eta}\sin\varphi, \tag{22}$$

$$V^{2\Omega} = A^{2\Omega}K_d^{2\Omega}\frac{\psi_d^2}{2}\sqrt{I_S^t I_R^t}\sqrt{\eta}\cos\varphi, \tag{23}$$

which correspond to the amplitudes of the corresponding harmonic terms, with $\psi_d = v_d K_{PZT}^{\Omega} \ll 1$ and $\Omega\tau_{sc} \gg 1$ [26]. The phase shift φ between the transmitted and diffracted beams behind the crystal is related (although not explicitly) to the hologram phase shift ϕ_p by Eqs. (4) and (8). The photodetector responses to Ω and 2Ω are K_d^{Ω} and $K_d^{2\Omega}$, with $K_d^{2\Omega} \approx K_d^{\Omega} = 13.9$ V m^2/W, respectively, and $K_{PZT}^{\Omega} = 0.057$ rad/V is the voltage-to-phase conversion at the phase-modulating device (a piezoelectric-supported mirror). I_S^t and I_R^t are the corresponding incident beams I_S^0 and I_R^0 measured at the crystal output (in the absence of any hologram) in order to avoid considering the effects of bulk absorption and surface reflections. The diffraction efficiency η and φ are computed from V^{Ω} and $V^{2\Omega}$ as follows:

$$\eta = \frac{1}{I_S^t I_R^t (K_d^{\Omega})^2}\left[\left(\frac{V^{\Omega}}{A^{\Omega}2v_d K_{PZT}^{\Omega}}\right)^2 + \left(\frac{2V^{2\Omega}}{A^{2\Omega}(v_d K_{PZT}^{\Omega})^2}\right)^2\right], \tag{24}$$

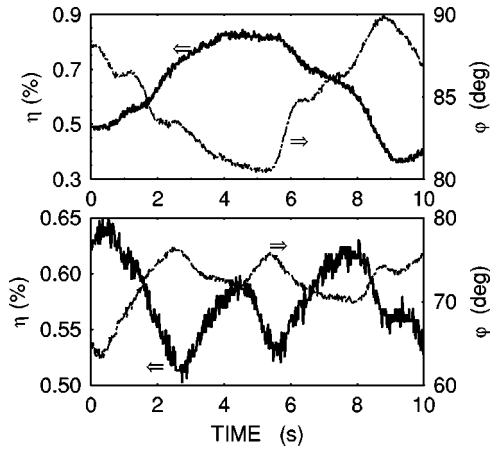

FIG. 3. Evolution of the computed η in percent (continuous thick curves) and φ in degrees (dashed thin curves) for positive gain (upper figure) with $I_S^0=0.38$ mW/cm^2 and for negative gain (lower figure) with $I_S^0=0.76$ mW/cm^2. A nominal field $E_0=7.3$ kV/cm is applied, the pump irradiance is $I_R^0=21.6$ mW/cm^2, and $\Omega=2\pi\times2000$ rad/s. The average over the 10-s period is $\overline{\eta}=(6.4\times10^{-3})\pm20\%$ for the positive and $\overline{\eta}=(5.8\times10^{-3})\pm6\%$ for the negative gain experiments shown here.

$$\varphi=\tan^{-1}\left[\frac{V^{\Omega}}{V^{2\Omega}}\frac{A^{2\Omega}}{A^{\Omega}}\frac{K_{\mathrm{PZT}}^{\Omega}v_d}{4}\right]. \tag{25}$$

B. Holographic recording under applied field

Two different experiments involving holographic recording under applied field were carried out, for negative and positive gain, using the same BTO sample: a stationary (nonmoving pattern of fringes) and a running (moving pattern of fringes) hologram experiment. Reversing the gain is just carried out by rotating the polarization of the input signal beam (I_S^0) direction by 90° and verifying that the sign of the energy transfer at the output is actually reversed.

1. Stationary hologram experiment

A stationary pattern of fringes was projected onto the crystal with a nominal applied dc field of 7.3 kV/cm. η and φ were measured, during a 10-s interval, as decribed above, for positive and for negative gain, and the data are shown in Fig. 3. Several experiments were carried out in these conditions, for $I_R^0\approx21.6$ mW/cm^2, and their results are displayed in Table I, where $\overline{\eta}$ and $\overline{\varphi}$ represent the corresponding averages whereas $\sigma_{\eta,\varphi}$ are the corresponding standard deviations computed in a 10-s range. Data from positive or negative gain are indicated by "pos." and "neg.," respectively. A representative example of data obtained from an experiment with negative gain and without applied field is also included in Table I. The analysis of data shows that η is much more unstable (see the fourth column in Table I) for the positive than for the negative gain experiment. In the absence of applied field, however, η is approximately as stable for positive as for negative gain ($\sigma/\overline{\eta}\approx0.04\approx0.03$, respectively, for $\beta^2=180$; not shown in Table I). A similar result ($\sigma/\overline{\eta}=0.025$) is shown in the last row in Table I, for $\beta^2\approx27$. Such different behavior for experiments with and without applied field indicates that the instability observed in the presence of field is not due to the setup itself but actually originates in the crystal under the effect of the field. The generation of transient running holograms [see Eq. (21)] excited by external perturbations may explain this behavior. In contrast with η, the phase φ is not noticeably affected (see last column in Table I) by the applied field or by the photorefractive gain being positive or negative. One possibility for such peculiar behavior may be that the noise on the phase in these experiments is predominantly produced by external perturbations (fast enough not to considerably affect η too) of the experimental setup. Such perturbations do directly act on the input beams, instead of arising from instabilities in the crystal itself, and therefore are just amplified along with the input signal and do not benefit from the noise reduction produced by the negative feedback. It should also be kept in mind that, although the effect of gain on the amplitude of the signal (that is to say, on the diffraction efficiency in our case) is clearly established for amplifying systems, there is no such simple relation for the phase. The parameter $(1+\beta^2)\eta$ in Table I is a kind of β^2-normalized η value, for the $\beta^2\gg e^{|\Gamma d|}$ condition [5,6], which better describes the influence of the gain sign on η.

TABLE I. Stability with positive and negative gain.

		Diffraction			Phase	
Gain	β^2	$\overline{\eta}$ (units of 10^{-3})	$\sigma_n/\overline{\eta}$ (%)	$(1+\beta^2)\overline{\eta}$	$\overline{\varphi}$ (deg)	σ_φ (deg)
		Under nominally applied field of 7.3 kV/cm				
pos.	56.7	4.6	18	0.26	87.2	1.7
pos.	56.7	6.4	23	0.36	84.9	2.9
pos.	56.7	5.6	27	0.32	85.1	3.7
neg.	28.3	5.8	8	0.16	71.4	2.8
neg.	28.3	5.8	6	0.16	72.2	2.9
neg.	28.3	5.8	5	0.16	71.4	2.3
neg.	28.3	5.4	5	0.15	73.2	1.9
		Without applied field				
neg.	26.7	5.8	2.5	0.16	1.17	2.0

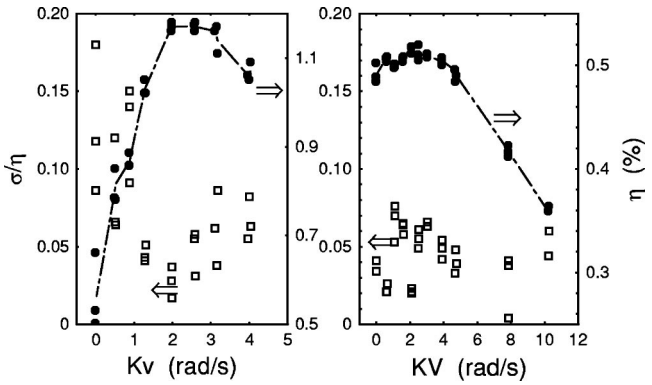

FIG. 4. Average diffraction efficiency in percent (circles) and standard deviation divided by average diffraction efficiency (squares) measured as a function of two-wave mixing detuning Kv in rad/s, for a positive gain with $K=4.87\ \mu\mathrm{m}^{-1}$, $\beta^2\approx 47$, and $I_R^0 \approx 13.3\ \mathrm{mW/cm}^2$ (left-hand side graphics) and for a negative gain with $K=2.55\ \mu\mathrm{m}^{-1}$, $\beta^2\approx 39$, and $I_R^0\approx 22\ \mathrm{mW/cm}^2$ (right-hand side graphics).

2. Running hologram experiment

To establish the effect of the gain on the stability of running holograms, two different experiments were carried out on the same sample, following the same schema described above and using the same measurement techniques. An experiment was carried out for negative gain, with $K=2.55\ \mu\mathrm{m}^{-1}$, $I_R^0=2.2\ \mathrm{mW/cm}^2$, and $\beta^2\approx 39$, and another one for positive gain with $K=4.87\ \mu\mathrm{m}^{-1}$, $I_R^0=13.3\ \mathrm{mW/cm}^2$, and $\beta^2\approx 47$. In both experiments a nominal field $E_0=7.3\ \mathrm{kV/cm}$ was applied to the sample. The average values $\overline{\eta}$ and $\sigma_n/\overline{\eta}$ (measured over a 10-s range, as for the stationary experiments above) are displayed, as a function of Kv, in Fig. 4 for positive (left-hand side graphics) and for negative (right-hand side graphics) gain. The detuning Kv is produced by a ramp voltage, of adequately chosen slope, applied to the same PZT-supported mirror used to produce the phase modulation of angular frequency Ω. It is interesting to verify that $\sigma_n/\overline{\eta}$ are, in general, considerably larger for the positive gain experiment than for the negative one. The positive gain experiment also shows a pronounced minimum of $\sigma/\overline{\eta}$ that roughly coincides with the maximum of $\overline{\eta}$, where resonance is achieved [see Eqs. (20) and (21)]. This fact may indicate that in these experiments the perturbations are associated with resonantly excited transient holograms of the type of Eq. (21). Such perturbations will be less noticeable as we approach resonance where larger steady-state running holograms are produced.

The transient effect discussed in Sec. III is clearly illustrated in Fig. 5 for running holograms. In this case a perturbation is automatically established by the starting of the ramp voltage (thick curve) applied to the PZT-supported mirror (in order to produce the necessary detuning Kv for the running hologram generation) in the setup. Figure 5 shows how fast the running hologram diffraction efficiency (thin curve) evolves to equilibrium after the setup is perturbed by starting the mirror movement. The negative gain experiment

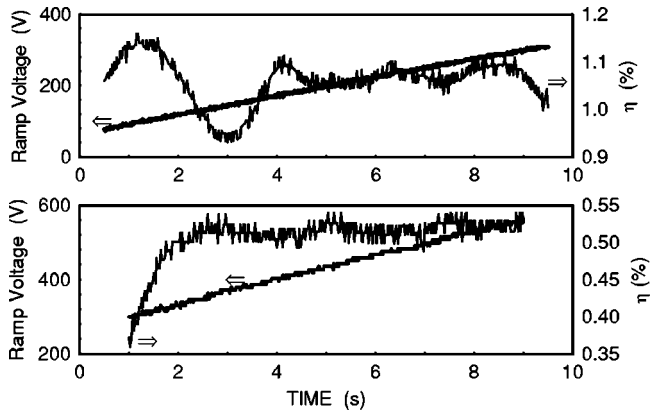

FIG. 5. Transient effect of a perturbation, in the form of a ramp voltage (thick curve) applied to the PZT-supported mirror in the holographic setup, upon the diffraction efficiency (thin curve) of a running hologram recorded in a photorefractive BTO crystal using the 514.4-nm wavelength. The diffraction efficiency evolution to equilibrium is faster for the negative gain (lower graphics, with $K=2.55\ \mu\mathrm{m}^{-1}$) than for the positive gain (upper graphics with $K=4.87\ \mu\mathrm{m}^{-1}$) experiment. Note that for the latter case the diffraction efficiency is still oscillating by the time the ramp voltage goes to the end. In both cases the applied external field is $E_0\approx 7.5\ \mathrm{kV/cm}$, the total incident irradiance is $I_0\approx 22.5\ \mathrm{mW/cm}^2$, and the beam ratio is $\beta^2\approx 40$.

(lower graphics) shows a much faster and less oscillatory evolution to equilibrium than the positive gain experiment in the upper graphics, in agreement with the theoretical predictions.

VI. CONCLUSIONS

In conclusion, we have confirmed the tradeoff between high diffraction efficiency and the instability exhibited by photorefractive (stationary and running) holograms under an applied electric field. On the basis of a simple comparison, we conclude that, as for electronic amplifiers, negative feedback should lead to more stable photorefractive holograms. We experimentally verify this statement at least as far as diffraction efficiency is concerned. Phase perturbations in the present experiment, however, exhibit a different behavior that deserves further research. Our results indicate that, in the present experimental conditions at least, noise probably arises from resonantly generated transient effects. We have also shown the possibility of phase modulation as a nonperturbative continuous measurement technique that is fully adapted to the highly Bragg-selective photorefractive volume holograms.

ACKNOWLEDGMENTS

We acknowledge the Conselho Nacional de Desenvolvimento Científico e Tecnológico and the Fundação de Amparo à Pesquisa do Estado de São Paulo for their financial support. We are thankful to the Laboratório de Crescimento de Cristais of the Instituto de Física de São Carlos at the Universidade de São Paulo for the crystal that enabled this research.

[1] D. L. Staebler and J. J. Amodei, J. Appl. Phys. **43**, 1042 (1972).
[2] D. von der Linde and A. M. Glass, Appl. Phys. **8**, 85 (1975).
[3] M. Peltier and F. Micheron, J. Appl. Phys. **48**, 3683 (1977).
[4] N. V. Kukhtarev, V. B. Markov, S. G. Odulov, M. S. Soskin, and V. L. Vinetskii, Ferroelectrics **22**, 949 (1979).
[5] J. Frejlich, P. M. Garcia, K. H. Ringhofer, and E. Shamonina, J. Opt. Soc. Am. B **14**, 1741 (1997).
[6] N. V. Kukhtarev, V. B. Markov, S. G. Odulov, M. S. Soskin, and V. L. Vinetskii, Ferroelectrics **22**, 961 (1979).
[7] P. Yeh, IEEE J. Quantum Electron. **25**, 484 (1989).
[8] J. Frejlich, A. A. Freschi, P. M. Garcia, E. Shamonina, V. Ya. Gayvoronsky, and K. H. Ringhofer, J. Opt. Soc. Am. B **17**, 1517 (2000).
[9] P. M. Garcia, K. Buse, D. Kip, and J. Frejlich, Opt. Commun. **117**, 235 (1995).
[10] H. V. Malmstadt, C. G. Enke, Jr., and E. C. Toren, *Electronics for Scientists* (Benjamin, New York, 1963).
[11] S. Stepanov and P. Petrov, *Photorefractive Materials and Their Applications I*, edited by P. Günter and J.-P. Huignard, Topics in Applied Physics Vol. 61 (Springer-Verlag, Berlin, 1988), Chap. 9, pp. 263–289.
[12] M. Cronin-Golomb, in *Digest of the Topical Meeting on Photorefractive Materials, Effects and Devices* (Optical Society of America, Washington, D.C., 1987), p. 142.
[13] M. Horowitz, D. Kligler, and B. Fisher, J. Opt. Soc. Am. B **8**, 2204 (1991).
[14] J. P. Huignard and F. Micheron, Appl. Phys. Lett. **29**, 591 (1976).
[15] S. Mallick, B. Imbert, H. Ducollet, J. P. Herriau, and J. P. Huignard, J. Appl. Phys. **63**, 5660 (1988).
[16] T. E. McClelland, D. J. Webb, B. I. Sturman, and K. H. Ringhofer, Phys. Rev. Lett. **73**, 3082 (1994).
[17] B. I. Sturman, A. I. Chemykh, E. Shamonina, V. P. Kamenov, and K. H. Ringhofer, J. Opt. Soc. Am. B **16**, 1099 (1999).
[18] B. I. Sturman, M. Mann, J. Otten, and K. H. Ringhofer, J. Opt. Soc. Am. B **10**, 1919 (1993).
[19] B. I. Sturman, E. V. Podivilov, A. I. Chemykh, K. H. Ringhofer, V. P. Kamenov, H. C. Pedersen, and P. M. Johansen, J. Opt. Soc. Am. B **16**, 556 (1999).
[20] Ivan de Oliveira and Jaime Frejlich, J. Opt. Soc. Am. B **18**, 219 (2001).
[21] V. V. Prokofiev, J. F. Carvalho, J. P. Andreeta, N. J. H. Gallo, A. C. Hernandes, J. Frejlich, A. A. Freschi, P. M. Garcia, J. Maracaiba, A. A. Kamshilin, and T. Jaaskelainen, Cryst. Res. Technol. **30**, 171 (1995).
[22] S. Mallick and D. Rouède, Appl. Phys. B: Photophys. Laser Chem. **43**, 239 (1987).
[23] T. J. Hall, R. Jaura, L. M. Connors, and P. D. Foote, Prog. Quantum Electron. **10**, 77 (1985).
[24] H. Kogelnik, Bell Syst. Tech. J. **48**, 2909–2947 (1969).
[25] A. A. Freschi and J. Frejlich, Opt. Lett. **20**, 635 (1995).
[26] S. Bian and J. Frejlich, Opt. Lett. **19**, 1702 (1994).